JGR Biogeosciences

RESEARCH ARTICLE
10.1029/2024JG008034

Divergent Responses of Organic Carbon to Sedimentary Environment Transformation in a River-Dominated Marginal Sea

Zhuoyue Zhang[1], Ming Lu[1], Chenglong Wang[1], Chuchu Zhang[1], Bingying Lin[2], Qihang Liao[1], Penghua Qiu[3], and Xinqing Zou[1,4]

[1]School of Geographic and Oceanographic Sciences, Ministry of Education Key Laboratory for Coast and Island Development, Nanjing University, Nanjing, China, [2]State Key Laboratory of Estuarine and Coastal Research, East China Normal University, Shanghai, China, [3]College of Geography and Environmental Science, Hainan Normal University, Haikou, China, [4]Collaborative Innovation Center of South China Sea Studies, Nanjing University, Nanjing, China

Abstract The fate of organic carbon (OC) in most river-dominated ocean margins (RiOMars) has undergone a noticeable transformation with the increased sediment retention engineering in watersheds. In the East China Sea (ECS), transformation in sediment and the influence of bulk OC have been broadly studied. However, the response of different mechanisms of OC protection under transformation has not been investigated, hindering our understanding of the factors that control OC deposition. In this study, we isolated different OC fractions, analyzed the basic parameters of the sediments, and compared the previous study's data to reveal how OC deposition responded to transformation. Our research indicates that transformation leads to the reduction of OC associated with minerals and sorting of OC occluded by plant debris and OC associated with minerals resulting in increased decomposition and mineralization of OC. The transformation affects the mechanism of OC binding with reactive iron (Fe_R), increasing Fe_R-protected OC content. Still, the co-precipitation mechanism and the intense redox environment in the mud deposit decrease the Fe_R-protected OC stability. Taken together, the impact of transformation is to increase the risk of OC decomposition and to weaken the OC preservation ability in RiOMars as carbon sinks. This study has implications for river-dominated passive margins subject to increased sediment retention engineering in watersheds worldwide and deserves more attention.

Plain Language Summary Many river-dominated ocean margins are changing because of human activities in the river basin. Scientists have studied how these changes affect sediment and organic carbon (OC) in the East China Sea. However, we still don't fully understand how different processes protect OC when sedimentary environments change. In our study, we researched various types of OC in the sediment and compared them with earlier research to explore how changes in sediment environments affect different types of OC. We found that as sediment environments change, the amount of OC associated with minerals decreases and the sorting of various types of OC, leads to uneven distribution of OC. The OC that binds with reactive iron (Fe_R) tends to increase, but its stability decreases in changing mechanisms and areas with intense chemical reactions. This study helps us understand how changes in sediment environments impact OC, which is important for similar regions around the world.

Key Points:

- Sedimentary environment transformation results in a mineral-associated organic carbon (OC) reduction and enhances OC decomposition
- Increased primary productivity leads to increased reactive iron co-precipitated with OC with relatively weak stability
- The impact of sedimentary environment transformation may weaken the preservation of OC worldwide and merits further attention

Supporting Information:

Supporting Information may be found in the online version of this article.

Correspondence to:

C. Wang and X. Zou,
clwang@nju.edu.cn;
zouxq@nju.edu.cn

Citation:

Zhang, Z., Lu, M., Wang, C., Zhang, C., Lin, B., Liao, Q., et al. (2024). Divergent responses of organic carbon to sedimentary environment transformation in a river-dominated marginal sea. *Journal of Geophysical Research: Biogeosciences*, *129*, e2024JG008034. https://doi.org/10.1029/2024JG008034

Received 24 JAN 2024
Accepted 21 OCT 2024

Author Contributions:

Conceptualization: Zhuoyue Zhang, Chenglong Wang
Data curation: Zhuoyue Zhang, Ming Lu, Bingying Lin
Formal analysis: Zhuoyue Zhang, Ming Lu, Chuchu Zhang, Qihang Liao
Funding acquisition: Xinqing Zou
Investigation: Zhuoyue Zhang, Chuchu Zhang, Qihang Liao
Methodology: Zhuoyue Zhang, Chenglong Wang, Qihang Liao
Software: Zhuoyue Zhang, Ming Lu, Bingying Lin
Supervision: Chenglong Wang, Xinqing Zou
Visualization: Zhuoyue Zhang
Writing – original draft: Zhuoyue Zhang
Writing – review & editing: Zhuoyue Zhang, Chenglong Wang, Chuchu Zhang, Bingying Lin, Xinqing Zou

1. Introduction

River-dominated ocean margins (RiOMars) influenced by large rivers, serve as major burial sites for terrestrial materials entering the ocean and experience significant interactions between rivers and sea (Bianchi & Allison, 2009; Gao & Collins, 2014; Gordon & Goñi, 2003). In response to the demands of human production and sustenance, there has been a progressive rise in the number of sediment retention engineering in watersheds, including dams and reservoirs (Milliman, 1997). The hydrodynamic and sedimentary characteristics in the RiOMars have undergone significant alteration (Gao et al., 2017). Sediment source-sink processes have been altered resulting in the estuarine delta being subjected to intense erosion (Gao et al., 2019; Wu et al., 2013; Yang et al., 2018). This has led to a considerable amount of fine-grained sediment being transported away from the estuary, thereby causing a notable increase in the coarseness of the sediments in the adjacent areas of the estuary (Gao et al., 2019; Wang, Hao, Feng, et al., 2020). This alteration in the integrated state of hydrodynamics,

sediment characteristics, and sediment source-sink processes is defined as sedimentary environment transformation.

The fate of organic carbon (OC) in RiOMars is influenced by various factors, especially hydrodynamics and sediment characterization (Blair & Aller, 2012). Sediment resuspension due to hydrodynamics alters the composition and flux of OC (Sun et al., 2024). Hydrodynamic processes affect OC's age, leading to OC aging during lateral migration (Bao et al., 2018). Less stable marine and terrestrial OC that is younger is more susceptible to selective decomposition, which can lead to the accumulation of older and more stable OC (Zhao et al., 2021). Transformations in the ability for OC adsorption are contingent upon alterations in sediment composition, which in turn permit modifications in the interaction between OC and minerals (Blair & Aller, 2012; Blattmann et al., 2019). Considering these factors are crucial for OC preservation and burial in RiOMars, sedimentary environment transformation greatly influences OC preservation and burial, which is very important to the global carbon cycle.

The East China Sea (ECS) has developed a very broad continental shelf, and a substantial amount of particulate organic matter is transported by the Changjiang River into the ECS (Wu et al., 2007; Yang et al., 2006), which provides an excellent repository for OC deposited. The sedimentary environment in the Changjiang River Estuary (CRE)-ECS Inner shelf region (ISR) has undergone significant transformation due to the increased construction of reservoirs and dams (Gao et al., 2017). The completion and operation of the Three Gorges Dam in 2003 served as a transformation year for the system. Thus, after 2003, the CRE-ECS ISR gradually entered a new system state (Gao et al., 2015). This has resulted in changes in the sources and a notable reduction of sediment and particulate OC transport into the sea (Gao et al., 2019; Wu et al., 2013; Yang et al., 2018). Conversion of sediment sources in the watershed and intensive human activities in the watershed has resulted in a significant amount of nutrient transport through the Changjiang River and into the ECS (Gao et al., 2018; Li et al., 2014). The decrease in sediment input leads to intensified erosion and resuspension in the CRE. As a result, sediment particles coarsen significantly, and surface sediments have transformed from uniformly fine-grained before the sedimentary environment transformation to the current pattern of coarse in the north and fine in the south (Gao et al., 2019; Wang, Hao, Feng, et al., 2020).

Thus far, the sedimentary characteristics and patterns of bulk OC under sedimentary environment transformation in the ECS have been extensively explored. Sedimentary environment transformation has profoundly influenced the deposition of OC in the ECS regarding temporal and spatial aspects. The hydrodynamic effects of the transformation mainly controlled the distribution of OC in the ECS, resulting in a 48% decrease in OC depositional fluxes (Wang, Hao, Gao, et al., 2020). The OC content in the CRE and adjacent shelves exhibited a general decline, with significant regional variations. Sediments are prone to sorting under hydrodynamic influences, and terrestrial OC exhibits distinct patterns of transport along shore or cross-shelf (Wang et al., 2022). The influx of substantial nutrient loads from terrestrial sources has caused severe eutrophication in the estuary and nearshore waters, which promotes the region's primary productivity and increases the contribution of marine OC (Gao et al., 2018; Li et al., 2014). In general, sedimentary environment transformation has affected the input, distribution, composition, age, and transport of OC in the ECS.

Nevertheless, these studies only discuss changes in bulk OC under sedimentary transformation and do not address changes in different preserved forms of OC. As research advances, it is becoming increasingly clear that various preserved OC forms have distinct fates in different environments. The deposition of OC in the ocean is influenced by both the physical occlusion of OC by plant debris and the chemical adsorption of OC by minerals (Blattmann et al., 2019; Sun et al., 2021). Several studies have investigated the fate of various OC fractions by distinguishing between sediments of different grain sizes and densities (Cui et al., 2016; Tesi et al., 2016; Wakeham et al., 2009). However, to distinguish between OC with different preservation mechanisms, further refinement of these distinctions is necessary. Therefore, to enhance the understanding of the interactions among different OC fractions in sediments and the mechanisms underlying the persistence of each fraction in different environments, researchers have classified bulk OC into three fractions with distinct characteristics: low-density particulate OC (LPOC), heavy-density particulate OC (HPOC), and mineral-associated OC (MAOC) (Cotrufo et al., 2019; Lugato et al., 2021). LPOC and HPOC are primarily found in coarse-grained sediments, and their preservation primarily depends on the short-term inhibition of plant debris and the barrier effect provided by occlusion. Consequently, their stability is lower, and they have a shorter mean residence time (Lavallee et al., 2020; Ye et al., 2018). In contrast, MAOC predominantly exists in fine-grained sediments, and its preservation primarily depends on

mineral-related physical and chemical processes, such as adsorption, chelation, and co-precipitation (Kleber et al., 2015; Lavallee et al., 2020). Preservation through mineral binding is generally stronger and longer-lasting than through other methods, resulting in higher stability and a longer mean residence time. The conceptualization of bulk OC as POC and MAOC is a well-supported and useful approach to processes of change in OC. This distinction between POC and MAOC provides a viable way to understand and predict changes in OC in the context of global change challenges.

Notably, reactive iron (Fe_R), defined as the iron phases in sediments extractable with sodium dithionite, which is widely distributed in the surface environment, has a complex formation and transformation mechanism (Chen et al., 2020; Lalonde et al., 2012; Vosteen et al., 2022). Owing to its strong ability to combine with OC, Fe_R plays a vital role in preventing OC decomposition, maintaining the stability of the marine sediment carbon pool, and regulating climate change (Faust et al., 2021; Lalonde et al., 2012; Shields et al., 2016). Although previous studies have described Fe-OC preservation in the CRE (Ma et al., 2018; Zhao et al., 2018, 2023), they have not involved the entire estuarine-inner shelf areas of the ECS and have lacked connections with the practical problems facing the ECS (e.g., reduction in terrestrial input and the change in hydrodynamic environment). Accordingly, OC preservation dominated by Fe_R in MAOC (Fe-OC), has been an important research subject in ECS OC preservation.

Against the backdrop of the sedimentary environment transformation, it is unclear how the synergistic effects of multiple factors, such as terrestrial input, mineral protection, and sedimentary dynamics affect the fate of OC during transport from the source. Therefore, it is of great significance to study the distribution and variation in different OC fractions (POC, MAOC, and Fe-OC) in the estuarine-inner shelf areas of the ECS, and the different OC fractions response to sedimentary environment transformation. In this study, we isolated different fractions from sediments in the ECS and measured the OC content and $\delta^{13}C$ of each fraction (LPOC, HPOC, MAOC, and Fe-OC), and combined some basic parameters of sediments previously analyzed (Wang et al., 2020a, 2020b) to explore the divergent responses of OC to sedimentary environment transformation in ECS. Through examining and analyzing the data and making comparisons with previous data, we sought to summarize a paradigm that describes the variations in different OC fractions, aiming to precisely understand and predict the OC deposition during sedimentary environment transformation in the estuarine-inner shelf areas of the ECS.

2. Materials and Methods

2.1. Overview of Study Area and Sampling

The study area is located between the CRE and the adjacent shelf (Figure 1a). The Changjiang River is the third largest river in the world, with a length of approximately 6.3×10^3 km and a basin area of 1.9×106 km^2 (Yao et al., 2015). The hydrodynamic conditions in the CRE and adjacent shelf are complex and mainly influenced by the Asian monsoon climate and boundary currents (Lee & Chao, 2003). The circulation system on the inner shelf of the ECS is intricate, with the Changjiang River Alluvial Diversion (CDW), the Zhejiang and Fujian Coastal Current (ZMCC), the Taiwan Warm Current, and the Kuroshio Current interacting to affect the migration, distribution, and deposition of sediments in the ECS (J. Liu et al., 2010). This circulation pattern impedes the transport of sediments across the shelf, resulting in the formation of extensive Mud deposits (MD) (J. P. Liu et al., 2006). As a result, a macroscopic transportation pattern of "summer storage and winter transmission" has formed in the near-shore area of the inner shelf (J. P. Liu et al., 2006). Changjiang River Estuary is located in the area to the north of 30°N latitude, based on the topography, circulation system, and depositional pattern (Wu et al., 2014). The sedimentary environment in the study area varies considerably from north to south and from MD to non-mud deposits due to the combined influence of human and natural factors. To investigate the impact of various sedimentary environments of OC in the north and south, we divided the sample sites' region into the CRE versus the ISR south of the estuary. Moreover, we divided the MD versus the NMD to investigate the impact of redox environments, formed by varying sediment types, on the deposition of OC (Figure 1b).

Three cruises were completed in the ECS onboard the R/V Kexue 3, R/V Xiangyanghong 18, and R/V Suruyu 08327 in March and May 2018. We collected 69 surficial sediment samples from estuary-inner shelf areas of the ECS using a box corer (Figure 1b). All sediment samples were stored at −20°C and then freeze-dried before laboratory analysis.

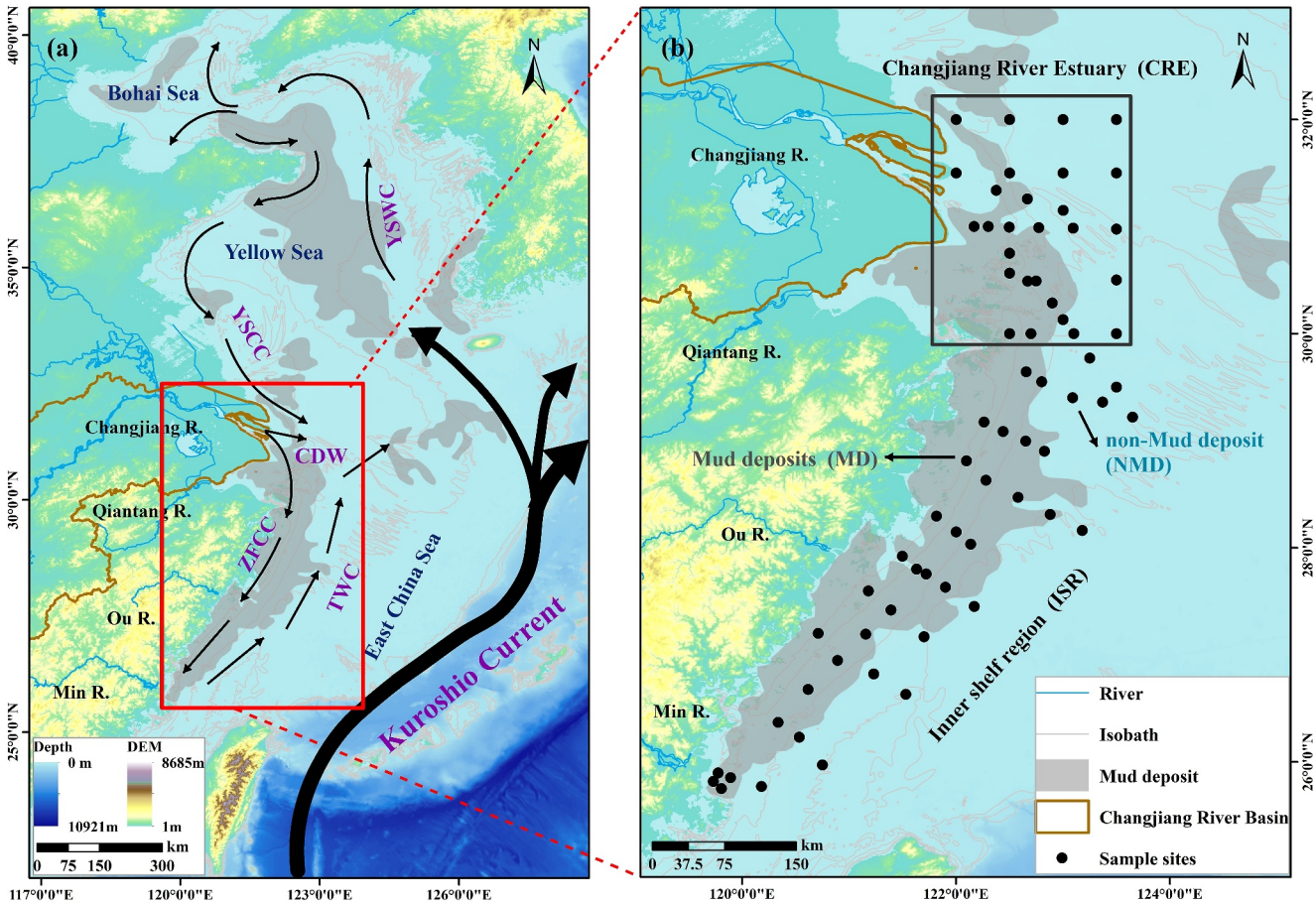

Figure 1. Study area in the East China Sea showing (a) black arrows are major oceanic currents redrawn from Wang et al. (2022) including the Changjiang-diluted water (CDW), Zhe-Min coastal current (ZMCC), Taiwan warm current (TWC), Yellow Sea coastal current (YSCC), Yellow Sea warm current (YSWC), and Kuroshio current (adapted from J. P. Liu et al., 2007). Gray patches are mud deposits that were redrawn by Gao et al. (2016). (b) Sampling sites in the Changjiang estuary and adjacent shelf.

2.2. Sedimentological Parameters

The grain size and specific surface area (SSA) of some of the samples were determined using the methods described by Wang, Hao, Feng, et al. (2020); Waterson and Canuel (2008), respectively. All samples were treated with an H_2O_2 solution (10%) to remove organic matter and then soaked in sodium metaphosphate for 24 hr to disperse the particles. The grain size was measured using a laser diffraction particle size analyzer (Mastersizer 2000, Malven Instruments Ltd., UK). The particle sizes were classified into three groups: clay (<4 μm), silt (4–63 μm), and sand (>63 μm). All freeze-dried sediments were heated at 350°C for 12 hr in a muffle furnace to remove organic matter, and then the SSA was measured using an automatic nitrogen adsorption surface area analyzer (BSD-PS4, Beishide Instrument-ST Co., Ltd., China). Some sedimentological parameters of the remaining samples were based on previously published data (Table S1 in Supporting Information S1) (Wang et al., 2020a, 2020b).

2.3. OC Fractionation

Various OC fractions have distinct formation pathways, chemical compositions, and protection mechanisms, as well as differing mean residence time (Figure 2). We combined the experiences of previous researchers and used the method of Lavallee et al. (2020), heavy liquid separation with wet sieving, to separate the low-density (LD), high-density and coarse (HD coarse), and high-density and fine (HD fine) fractions. First, a 5g sediment sample was added into a centrifuge tube, then added 25 ml of $ZnCl_2$ with a density of 1.6 g cm^{-3}, and mixed thoroughly. Second, after ultrasonic treatment, the mixture was centrifuged at 1,800 × g, and the upper suspension was filtered

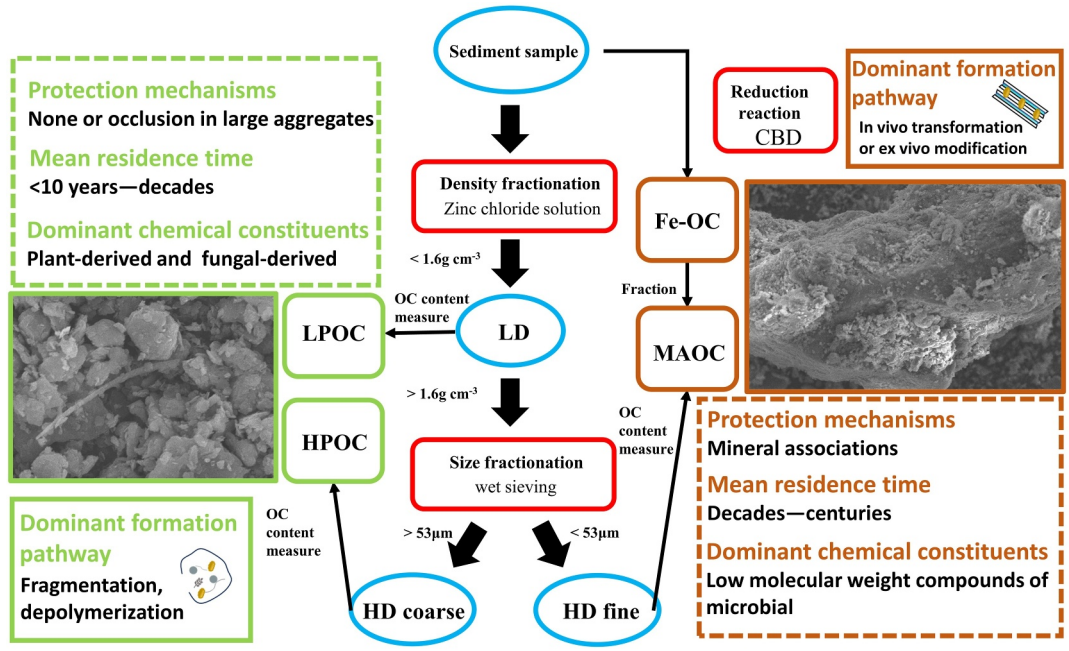

Figure 2. The isolated and extracted procedure of different density and particle size sediments. The method and description of the different organic carbon (OC) fractions come from Lavallee et al. (2020). The SEM was used to capture photographs of the various fractions of OC shown in the figure. The POC and MAOC samples correspond to CJK2-1 and b44, respectively.

using a GF/C filter membrane, rinsed with deionized water, and then freeze-dried. The OC content in this separated fraction (LD) is the LPOC. Finally, after rinsing the mixture in the tube with deionized water, we used a 53-μm sieve for separation, and then freeze-dry the separated components separately. The OC content of the fraction (HD coarse) remaining on the sieve (<53 μm) is called HPOC, and the fraction (HD fine) passing through the sieve (>53 μm) is called MAOC (Figure 2). Freeze-dried samples were reacted with 1M HCl for 24 hr, and then washed with deionized water until neutral and then dried. The Thermo Flash 2000 Elemental Analyzer interfaced with a MAT-253 isotope ratio mass spectrometer was used to determine OC content and $\delta^{13}C$ of each fraction. The precision of OC determination for sediment samples is better than ±0.02 wt.% ($n = 276$). Bulk OC, POC, MAOC, and Fe-OC were calculated by the following equations:

$$\text{POC}\ (\%) = \text{OC}_{\text{LD}} \times \text{f}_{\text{LD}} + \text{OC}_{\text{HD coarse}} \times \text{f}_{\text{HD coarse}} \quad (1)$$

$$\text{MAOC}\ (\%) = \text{OC}_{\text{HD fine}} \times \text{f}_{\text{HD fine}} \quad (2)$$

$$\text{Bulk OC}\ (\%) = \text{POC} + \text{MAOC} \quad (3)$$

$$\text{Fe-OC}\ (\%) = \text{OC}_{\text{control}} - \text{OC}_{\text{extract}} \quad (4)$$

where OC_{LD}, $OC_{HD\ coarse}$, and $OC_{HD\ fine}$ are the OC content for the fractions of LD, HD coarse, and HD fine, respectively. f_{LD}, $f_{HD\ coarse}$, and $f_{HD\ fine}$ are the percentages of the total mass for the fractions of LD, HD coarse, and HD fine, respectively. $OC_{control}$ is the OC content in the Fe extraction control experiment and $OC_{extract}$ is the OC content after the Fe extraction experiment.

$\delta^{13}C$ of Bulk OC, POC, MAOC, and $\delta^{13}C_{Fe\text{-}OC}$ were reported in a unit of per million (‰) as follows:

$$\delta^{13}\text{C} = \left(\frac{\text{R}_{\text{sample}}}{\text{R}_{\text{standard}}} - 1\right) \times 1000 \quad (5)$$

$$\delta^{13}\text{C}_{\text{Fe-OC}} = \frac{\delta^{13}\text{C}_{\text{control}} \times \text{OC}_{\text{control}} - \delta^{13}\text{C}_{\text{extract}} \times \text{OC}_{\text{extract}}}{\text{OC}_{\text{control}} - \text{OC}_{\text{extract}}} \quad (6)$$

where R_{sample} and $R_{standard}$ are the ratios of $^{13}C/^{12}C$ for the sample and standard, respectively. $\delta^{13}C_{control}$ is the $\delta^{13}C$ in the Fe extraction control experiment and $\delta^{13}C_{extract}$ is $\delta^{13}C$ after the Fe extraction experiment. $\delta^{13}C$ values were reported using the standard notation relative to the Vienna Pee Dee Belemnite standard. The analytical precision was better than ±0.1‰ based on replicate measurements.

The determination of Fe_R and Fe-OC used the bicarbonate-citrate buffered dithionite (BCD) reduction method by Mehra and Jackson (2013) as modified by Lalonde et al. (2012). We divided the samples into a treatment group and a control group. Then 0.27 M trisodium citrate, 0.11 M sodium bicarbonate, and 0.1 M sodium dithionite were added to the treatment group to extract Fe_R and Fe-OC from the sample. The control group was treated with the same ionic concentration of NaCl instead of trisodium citrate and sodium dithionite. Fe_R has been extracted into the upper layer solution of the treatment group and Fe_R was measured by inductively coupled plasma optical emission spectrometer (iCAP6300, Thermo Fisher Scientific., USA). The difference in OC content between the two groups is OC-Fe content. Because the content of separated LPOC fractions is very low compared with other fractions, and LPOC has similar properties to HPOC (Lavallee et al., 2020), the two fractions of LPOC and HPOC were combined and analyzed together, and are referred to as POC hereafter.

2.4. Data Collection

The paucity of POC and MAOC studies in the ocean makes it challenging to directly collect POC and MAOC data for comparison before the sedimentary environment transformation. However, there are more studies on separating as well as measuring OC from different sediment types in the ocean based on water elutriation. The water elutriation was separated according to the different grain sizes of the sediments using the wet sieve method (He et al., 2010). Thereafter, the OC content in the different grain size classifications was tested. The 63 μm grain size partition is a significant criterion for differentiating between various sediment types. The 63 μm grading also exhibits a degree of responsiveness to the distinction between plant detritus and OC associated with minerals (Sun et al., 2021). Based on our data, we found that the grain size range distribution of 53–63 μm accounts for less than 4% of the total, and the error in 53–63 μm sediment fractions in the ECS is low (Table S5 in Supporting Information S1). Therefore, given the dearth of high-density fraction content in the ECS and the findings of prior studies on the OC fractions, it is reasonable to hypothesize that POC is analogous to the high-size fraction OC (>63 μm), whereas MAOC is analogous to the low size fraction OC (<63 μm). To facilitate a comparison between POC and MAOC in the context of the sedimentary environment transformation, we have collated data on OC for particles >63 μm as well as <63 μm ($n = 51$) from previous studies based on water elutriation (Table S6 in Supporting Information S1) (Bao et al., 2019; Ji et al., 2020; H. Liu et al., 2017; Pan, 2016; Pan et al., 2015, 2016b; Wang et al., 2015).

In order to examine the response of Fe-OC to the sedimentary environment transformation, Fe_R, Fe-OC, Fe-OC fraction ($f_{Fe\text{-}OC}$), and OC/Fe molar ratio data ($n = 50$) was collected from the previous research in the different regions of ECS, with a view to undertaking a comparative analysis (Ma et al., 2018; Zhao et al., 2018). To ensure the comparability of the data, the experimental methods employed in the previous study must be the same in this study.

2.5. Statistical Analyses

All data analyses were performed using SPSS software (version 22.0; SPSS Institute, USA). Pearson's correlation analysis and two-tailed tests were used to determine the correlations among all measured parameters. Based on a 95% confidence interval, significant statistical differences were determined using *t*-tests.

3. Result

3.1. Basic Parameters of the Bulk Sediments

The bulk properties of the surface sediments estuarine and inner shelf areas of the ECS are shown in Table S2 in Supporting Information S1. The mean grain size (Mz) ranged from −0.43 Φ to 7.09 Φ with a mean of 4.79 ± 2.26 Φ. The Mz in ISR (5.70 ± 1.41 Φ) was significantly higher than those in CRE (3.46 ± 2.64 Φ) ($p < 0.05$). The Mz of MD (5.40 ± 1.90 Φ) is significantly higher than those in NMD (3.65 ± 2.50 Φ) ($p < 0.05$). This demonstrates that sediment grains are the coarsest in the CRE and relatively coarse in the NMD, while the MD and ISR are primarily composed of fine-grained sediments. Concerning the sediment type, clay accounted for 14.24 ± 6.38%

of total sediment, and silt accounted for 76.86 ± 16.86%. The lowest percentage was observed in the sand sediment, at 8.90 ± 16.60%. The surface sediment was mainly composed of silt and clay in ISR, and mainly composed low proportion of sand in CRE. The surface sediment was mainly composed of silt and clay in MD, and mainly composed low proportion of sand in NMD. The SSA values of surface sediments ranged from 3.24 to 24.9 m^2/g with an average of 15.54 ± 7.01 m^2/g. The SSA of CRE (5.70 ± 2.64 m^2/g) is significantly lower than that of ISR (17.46 ± 6.13 m^2/g) ($p < 0.05$). The SSA of MD (18.38 ± 5.93 m^2/g) is significantly higher than NMD (12.73 ± 7.49 m^2/g) because of the differences in sediment types ($p < 0.05$). In general, the sediments with fine particles and strong adsorption ability were mainly concentrated in MD and ISR, and the NMD and CRE were mainly coarse particles and a low adsorption ability for substances.

3.2. Bulk OC and OC Fractions

The properties of various OC fractions in the estuarine inner shelf of the ECS are shown in Tables S3 in Supporting Information S1. The bulk OC content ranged from 0.09% to 0.90% with a mean of 0.53 ± 0.18%, and the value of MAOC ranged from 0.01% to 0.81% with a mean of 0.46 ± 0.20%. The POC content (POC = LPOC + HPOC, 0.07 ± 0.06%) ranged from 0.01% to 0.28%, which was relatively low. Bulk OC and MAOC had similar spatial distribution characteristics, with both having high content in the MD (0.58 ± 0.16% and 0.54 ± 0.17%) and ISR (0.61 ± 0.10% and 0.55 ± 0.12%) and the low content was in the NMD (0.45 ± 0.18% and 0.33 ± 0.18%) and CRE (0.42 ± 0.21% and 0.33 ± 0.22%) (Figures 3a, 3c, and 4). POC had the opposite distribution to MAOC, having a high content in the NMD (0.13 ± 0.06%) and CRE (0.09 ± 0.07%) and low content in the MD (0.04 ± 0.04%) and ISR (0.06 ± 0.06%) (Figures 3b and 4). The average fractions of POC and MAOC to bulk OC were 19.80 ± 24.87%, 80.20 ± 24.87%, respectively (Figures 3f–3h). In the CRE, POC represents the predominant fraction of OC, whereas, in MD, MAOC is the predominant fraction of OC. The bulk $\delta^{13}C$ values ranged from −25.6‰ to −21.4‰ with an average of −22.47 ± 0.69‰. The average values of $\delta^{13}C_{POC}$, and $\delta^{13}C_{MAOC}$ were determined to be −22.95 ± 1.08‰, and −22.57 ± 0.65‰, respectively. They were more depleted in the MD and CRE and less depleted in the NMD and ISR (Figures 3i–3k). Overall, the $\delta^{13}C$ signal gradually depletes from sea to continent.

There was significant relationships correlation between bulk OC and basic sediment parameters (Mz, SSA, Silt, and Clay) throughout the entire surface samples ($R = 0.81$, $p < 0.001$; $R = 0.66$, $p < 0.001$; $R = -0.37$, $p < 0.001$; $R = 0.67$, $p < 0.001$; Figure 5). Similarly, there were significant relationships correlation between MAOC and basic sediment parameters (Mz, SSA, and Clay) throughout the entire surface samples ($R = 0.83$, $p < 0.001$; $R = 0.78$, $p < 0.001$; $R = 0.75$, $p < 0.001$; Figure 5). The correlation between POC and basic sediment parameters differs from that observed in the bulk OC and MAOC. There was a significant relationship correlation between POC and basic sediment parameters (Mz, SSA, Silt, and Clay) throughout the entire surface samples ($R = 0.81$, $p < 0.01$; $R = 0.66$, $p < 0.001$; $R = -0.37$, $p < 0.01$; $R = 0.67$, $p < 0.001$; Figure 5).

3.3. Fe-OC Associations

The value of Fe_R ranged from 18.76 to 114.85 μmol/g with a mean of 57.09 ± 21.85 μmol/g and the distribution of Fe_R decreased as the distance from the shore increased (Figure 3e). Fe_R has a significant negative correlation with latitude and longitude ($p < 0.001$; Figures 6a and 6d). Fe-OC (0.08 ± 0.06%) ranged from 0.01% to 0.23% and was higher in ISR and NMD, whereas it was relatively low in other regions (Figure 4b). There were no significant relationships between Fe-OC and basic sediment parameters throughout the entire surface samples ($p > 0.05$; Figure 5). No significant correlation was observed between Fe-OC and either latitude or longitude ($p > 0.05$; Figures 6b and 6e). The average fractions of Fe-OC to bulk OC were 16.28 ± 10.98%. There is a relative increase in the role of Fe-OC in NMD (Figure 3h). The value of $\delta^{13}C_{Fe\text{-}OC}$ was different from POC and MAOC, ranging from −33.88‰ to −19.17‰, with a mean of −24.79 ± 3.51‰. The $\delta^{13}C_{Fe\text{-}OC}$ is depleted more significantly than the other components and gradually depletes from sea to continent as well. Unlike the distribution patterns observed in the POC and MAOC, it exhibited a strong terrestrial source signal. The ratio of OC to Fe_R can indirectly indicate how the Fe_R binds to the OC. Generally, when OC/Fe < 1, the main binding mode is adsorption and the OC/Fe ratio of binding through coprecipitation typically ranges from 6 to 10 (Wagai & Mayer, 2007). The mean value of OC/Fe in our study area is 1.40 ± 1.40, indicating a mixture of adsorption and coprecipitation binding. No significant correlation was observed between OC/Fe and either latitude or longitude ($p > 0.05$; Figures 6b and 6e).

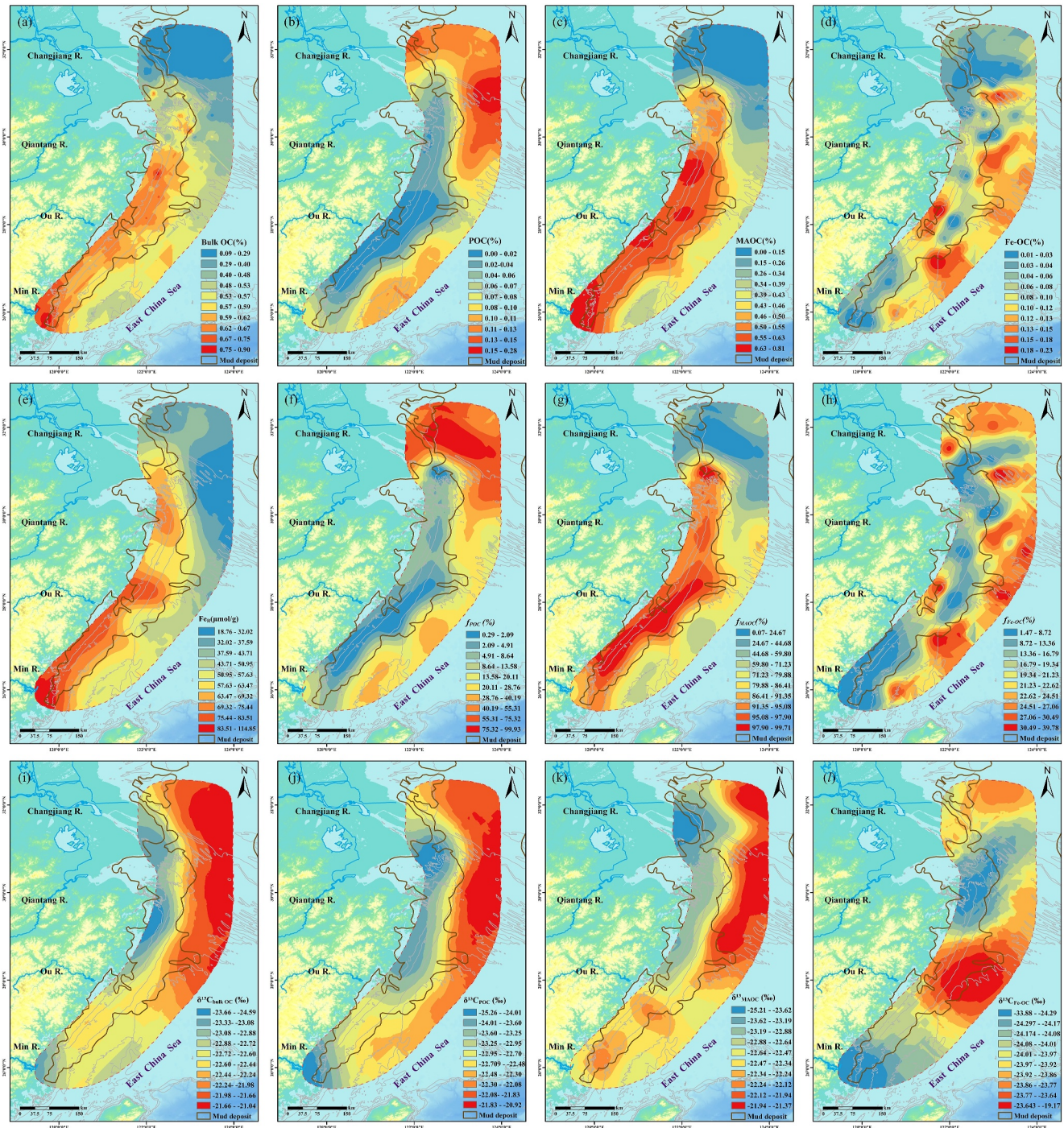

Figure 3. Distributions of various fractions of organic carbon (OC) in surficial sediments from the estuarine-inner shelf areas of the ECS; (a–d) various fractions of OC content, (e) Fe_R content, (f–h) fraction of various fractions of OC, and (i–l) various fractions of $\delta^{13}C$.

4. Discussion

4.1. Characterizing the Different OC Fractions Under the Sedimentary Environment Transformation

Past work suggested that the impounding of the Three Gorges Reservoir commenced in 2003, which marked the inception of the sedimentary environment transformation (Gao et al., 2015). However, at this time, the impact on the source-sink processes of sediments in the Changjiang River Basin is still relatively limited. In 2012, the

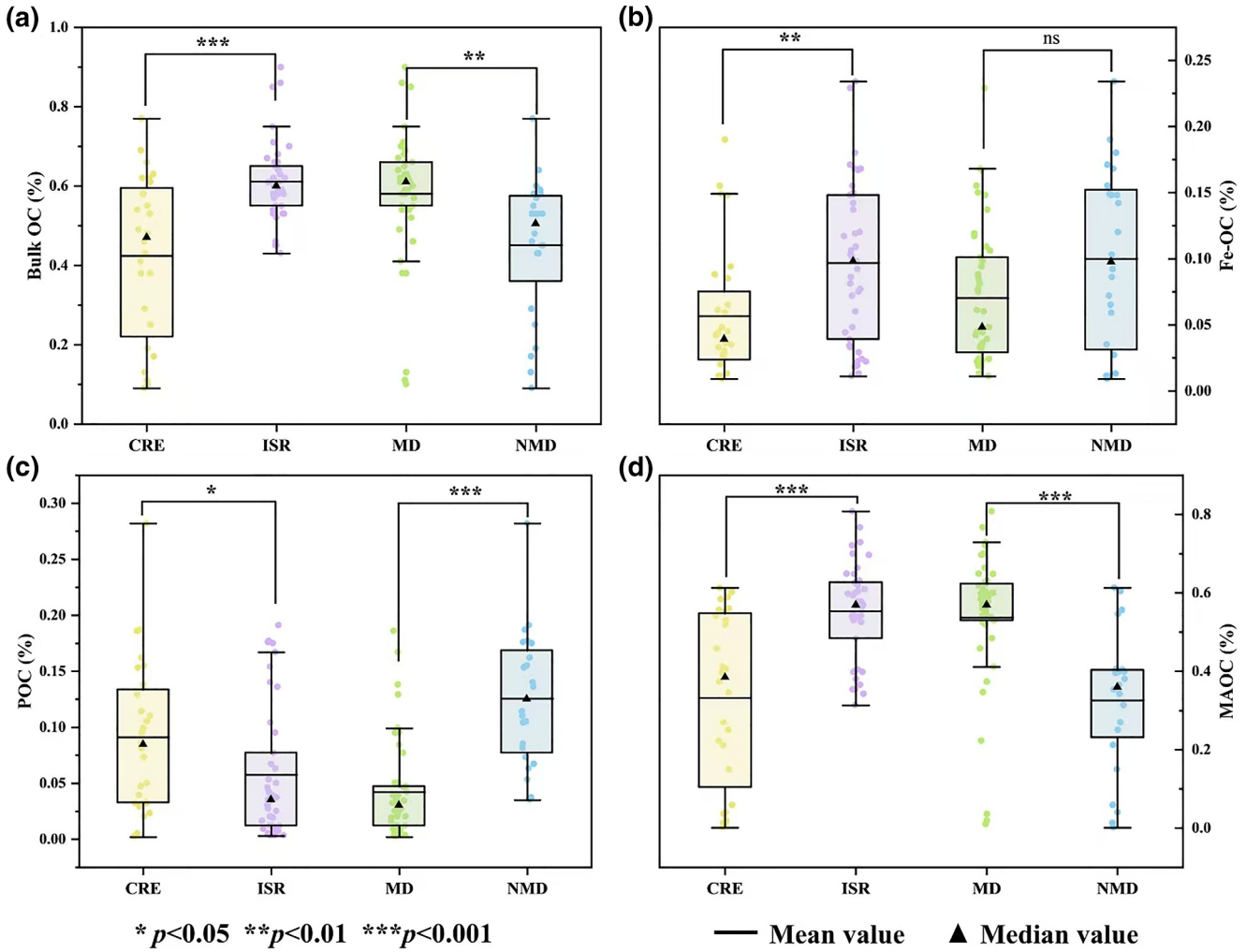

Figure 4. Comparison of various organic carbon fractions in different regions of the ECS; (a) Bulk OC; (b) Fe-OC; (c) POC; (d) MAOC. The star symbol represents the significance of the difference test in different regions. The upper and lower edges of the box respectively indicate the 25% and 75% percentiles of the data.

construction of all upper Changjiang River terrace reservoirs was completed, resulting in an interception rate of nearly 100% of upstream sediment in the basin's reservoirs (Gao et al., 2018). Sedimentary environments in the estuary and adjacent shelf have gradually changed since 2012 (inlet fluxes are more sensitive, while sediments are pushed back by 3–5 years to respond to the system transformation) (Gao et al., 2019; Wu et al., 2013). The transformation is an ongoing state that has been intensifying since 2012. The impact of sedimentary environment transformation on OC preservation can be explored by a comparative analysis of data from different periods before and after.

The process of reservoir interception serves to diminish the flux of sediment to the sea, in addition to reducing the input of bulk OC to the sea (Wang, Hao, Gao, et al., 2020; Wu et al., 2013; Yang et al., 2018). After comparing the data with the previous data (Figure S1 in Supporting Information S1), we concluded that sedimentary environment transformation also has a direct impact on spatial distribution patterns due to the enhanced erosion and resuspension in CRE (Wang, Hao, Feng, et al., 2020). The sediment grain size shifted from uniformity before the sedimentary environment transformation to a recent pattern of coarser sediments in the north and finer sediments in the south (Figure S1 in Supporting Information S1). Similarly, the characterization of bulk OC changed from high content and uniform distribution to low content and significant north-south differences (Wang, Hao, Feng, et al., 2020). The reduction in MAOC and the variability of POC and MAOC over different regions could provide support for this conclusion and dig deeper into the factors (Figure 7). In the CRE, the sedimentary environment

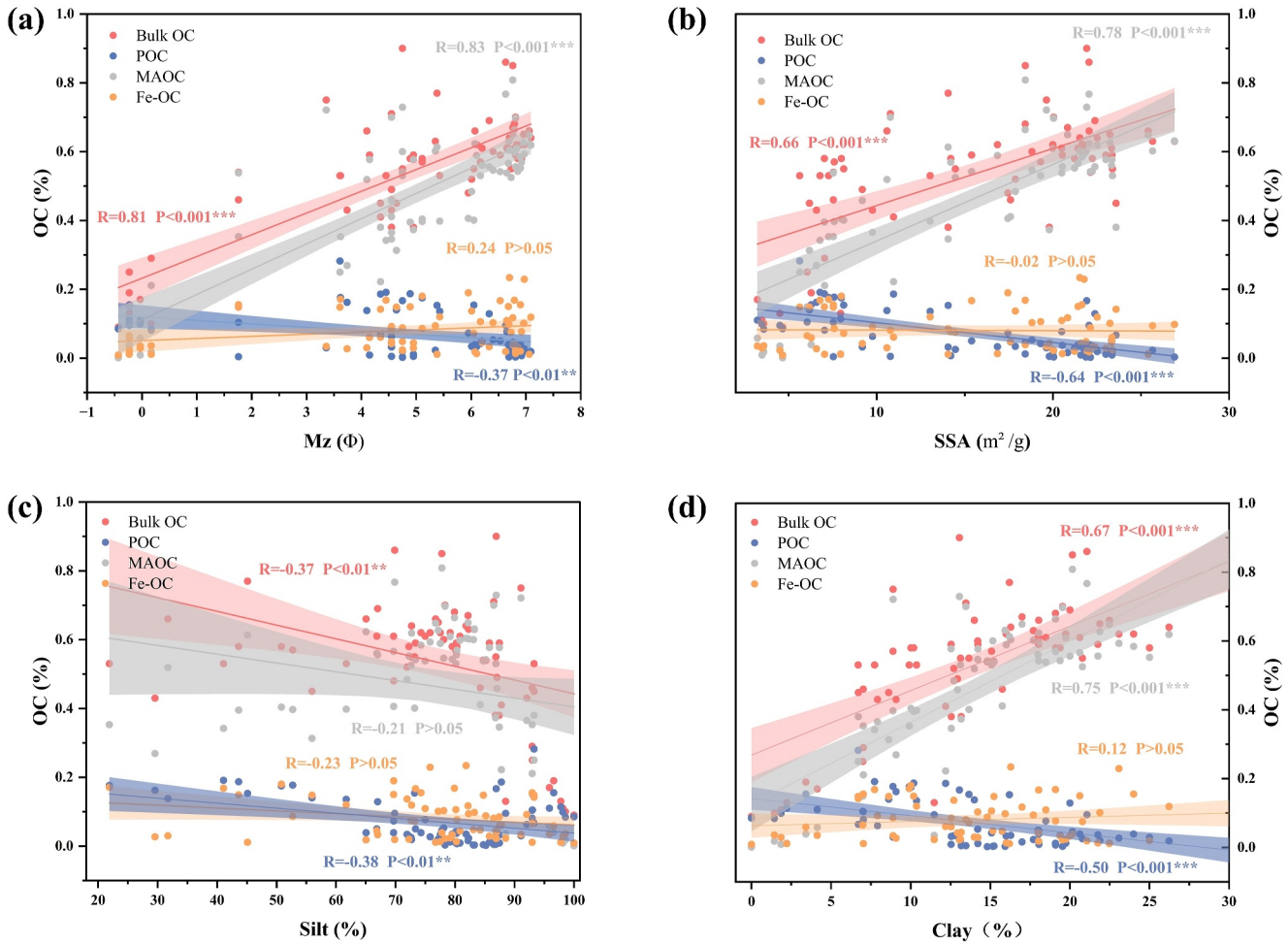

Figure 5. Correlations between various basic sedimentary parameters and various fractions of OC; (a) Correlations between mean grain size (Mz) and various fractions of OC; (b) Correlations between mean specific surface area and various fractions of OC; (c) Correlations between silt and various fractions of OC; (d) Correlations between clay and various fractions of organic carbon.

transformation resulted in an increase in the content and percentage of POC and a decrease in the content and percentage of MAOC. In contrast, in the ISR, the change was not significant ($P > 0.05$) (Figures 7c and 7d). However, due to the limited data set in the ISR, the MAOC in the ISR region before the sedimentary environment transformation may have been underestimated. In MD and NMD, the content and percentage of MAOC decreased slightly, while the content and percentage of POC increased (Figures 7c and 7d). Overall, the alteration in POC after the sedimentary environment transformation was not considerable, exhibiting only a slight increase in content, while MAOC content decreased by approximately 20% (Figure 7b).

This is because POC is more prevalent in coarse-grained sediments, whereas MAOC is predominantly found in fine-grained sediments (Figure 5). The enhanced erosion of CRE results in the resuspension of fine-grained sediments (Sun et al., 2021, 2024), thereby increasing the exposure time of MAOC to oxygen and consequently elevating the risk of MAOC decomposition and mineralization. Moreover, Under the influence of hydrodynamics, POC and MAOC underwent significant sorting in CRE (Figures 3f and 3g). The sorting effect gives rise to a spatial distribution pattern of high POC in CRE and high MAOC in ISR and MD. It is worth noting that increased nutrients may also be a contributing factor to the increased POC content. As a result, sedimentary environment transformation alters the content and spatial distribution of different OC forms by decreasing terrestrial inputs and modifying the hydrodynamic environment. Notably, Fe-OC does not increase with Fe_R (Figures 3e and 3h), nor does it correlate directly with sedimentological parameters (Figure 5). The control factors

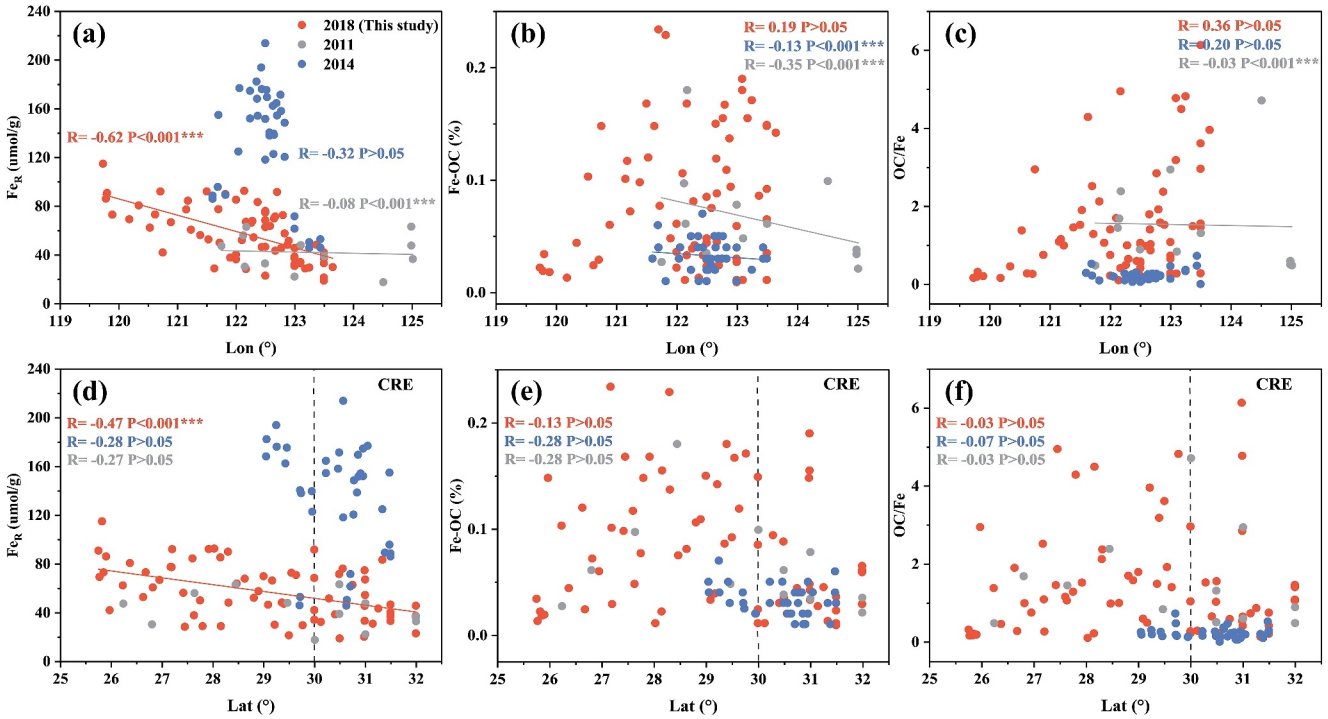

Figure 6. Temporal and spital variations in Fe_R, Fe-OC, and organic carbon (OC)/Fe; Data in red represent data from this study, the sampling year 2018; Data in blue represent data from Zhao et al. (2018), the sampling year 2014; Data in gray represent data from Ma et al. (2018), the sampling year 2011; (a–c) Correlations between Fe_R, Fe-OC, OC/Fe and longitude; (d–f) Correlations between Fe_R, Fe-OC, OC/Fe and latitude.

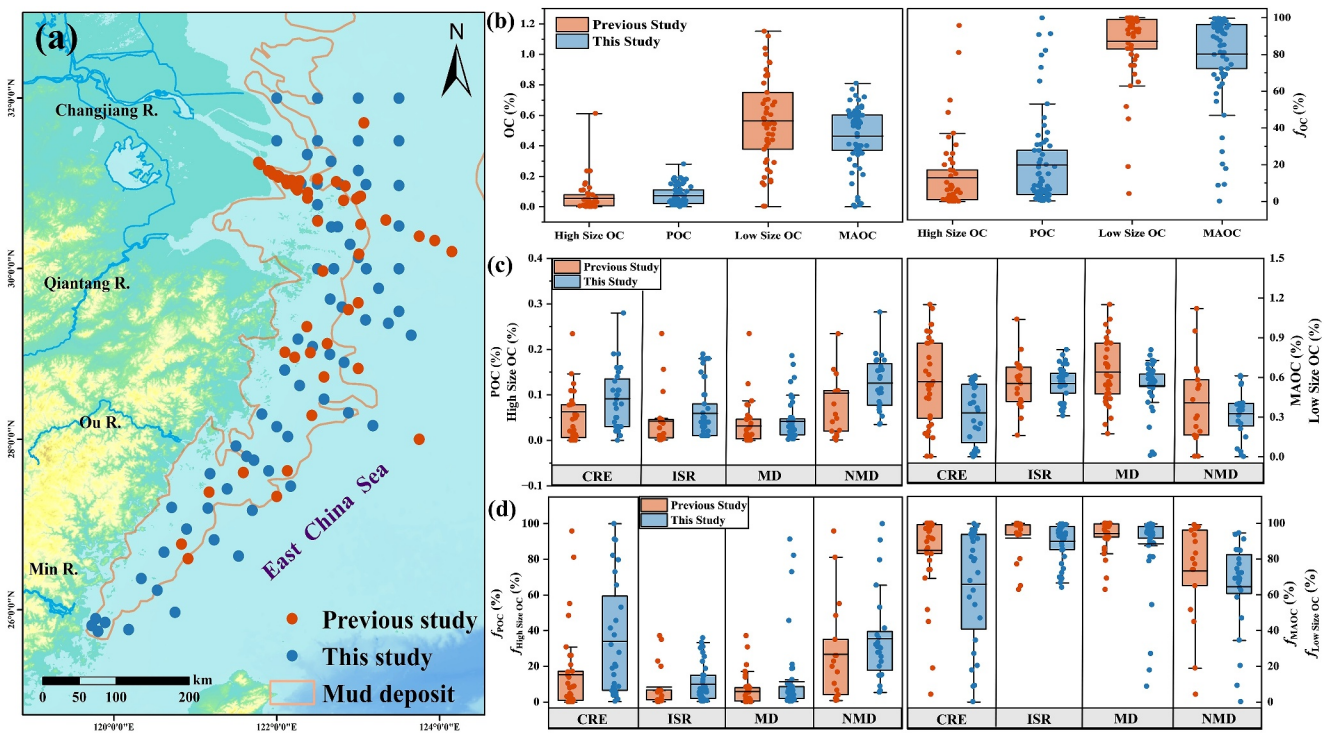

Figure 7. Temporal and regional variations in POC and MAOC under sedimentary environment transformation; (a) Sample sites of data in the previous study and this study; (b) Comparison of various organic carbon (OC) fractions in the previous study and this study; (c) Comparison of various OC content of the previous study and this study in different regions of the ECS; (d) Comparison of various OC contribution of previous study and this study in different regions of the East China Sea.

of Fe-OC under sedimentary environment transformation appear to be relatively specific and are further discussed below.

4.2. The Unique Control Factors of Fe-OC Under Sedimentary Environment Transformation

The mechanisms and factors affecting the binding of Fe_R to OC are highly complex because of the properties of the variable-valence metal (Chen et al., 2020). One potential control on Fe-OC is the source and content of Fe_R. Different sources of Fe_R have different properties, in particular the degree of crystallinity which is essential for the binding of Fe_R to OC (Chen et al., 2020). Furthermore, the source of OC also exerts a significant impact on the formation of Fe-OC. The Fe_R exhibits a proclivity for binding OC derived from different sources, with a greater affinity for terrestrial OC through adsorption and marine OC through co-precipitation (Hu et al., 2023). The Fe_R binding OC through adsorption is more stable, while Fe_R binding OC through co-precipitation is more abundant (Hu et al., 2023). The distinction between the two binding mechanisms is that the former involves the interaction of OC with the surface after the formation of ferric oxides from free iron, while the latter involves the co-precipitation of the two during the formation of oxides from free iron due to the presence of OC interfering with its crystal growth (Hu et al., 2023). In addition, the effect of the redox environment on Fe-OC cannot be ignored. The protective effect of Fe_R on OC is enhanced in more stable redox environments, whereas vigorous redox environments have the opposite effect (Chen et al., 2020; Zhao et al., 2018). In conclusion, Fe-OC is shaped by a complex interplay of Fe_R and OC sources, redox environments, and other variables.

The Fe_R inputs, primarily from terrestrial sources (Shields et al., 2016), are subject to sedimentary environment transformation. Fe_R input in ECS decreases after sedimentary environment transformation (Figures 6a and 6d). It gradually decreases from the continent toward the sea (Figure 3e). However, there is a spatially and temporally mismatch in ECS between Fe_R and Fe-OC (Figures 3d–3f, 6b, and 6e). We suggest that the decreased Fe_R but increased Fe-OC after sedimentary environment transformation concerns the binding mechanisms of different OC sources. Sedimentary environment transformation has led to more nutrients entering the CRE, higher levels of primary productivity, and increased OC content from marine sources (Li et al., 2014). Fe_R is biased to bind marine OC by co-precipitation, which binds more OC (Hu et al., 2023; Figure S2 in Supporting Information S1), as indicated by the increased OC/Fe and less depleted $\delta^{13}C_{Fe\text{-}OC}$ in CRE (Figures 6c and 6f). As the signal strength of the marine source increases with distance offshore (Figure 3i), co-precipitation emerges as a crucial mechanism for understanding the interactions between Fe_R and OC (Figures 6c and 6f). Notably, the co-precipitation mechanism results in a reduction in the stability of Fe-OC (Hu et al., 2023).

The varying redox environments across different regions influence the spatial distribution of Fe-OC. For example, the MD with an intense redox environment can have counteractive effects on OC preservation (Chen et al., 2020; Zhao et al., 2018). This intense redox environment can increase the maturation and crystallization of iron oxide (Sheng et al., 2021), which can result in a decreased ability to preserve OC. Accordingly, the Fe-OC preserved in a strong redox environment such as MD is very limited (Zhao et al., 2018). The NMD shows an increase in the ability of Fe_R to bind OC due to the stabilization of the redox environment in this region. It is likely that free Fe_R is transported here and binds OC by co-precipitates at the sediment interface leading to a significant increase in the protective effect of Fe_R on OC in this region (Figures 3d and 3h). Accordingly, the Fe-OC content in a stable redox environment such as NMD is relatively high and is a large number from marine sources.

In general, the sedimentary environment transformation has resulted in a decrease in Fe-OC from terrestrial sources and an increase in Fe-OC from marine sources. The OC content increased in ECS but the OC preservation ability of Fe_R may weaken under sedimentary environmental transformation. Although Fe_R does not dominate OC preservation in frequent redox environments, in areas where the redox environment is stable, the role of Fe_R in preserving OC increases (Chen et al., 2020). This implies that the interaction between Fe_R and OC is influenced by regional chemical environments, source of OC, and functional groups (Hu et al., 2023). Understanding the unique control factors of OC to Fe_R is crucial for studying the long-term OC preservation by Fe_R in ECS.

4.3. Response of Different OC Fractions to Sedimentary Environments Transformation and Its Global Implications

After the sedimentary environment transformation in the ECS, each fraction of OC has distinct depositional characteristics in different regions and under different environments. Our study proposes a paradigm for the change of OC fractions after sedimentary environment transformation (Figure 8). The decrease in inputs from

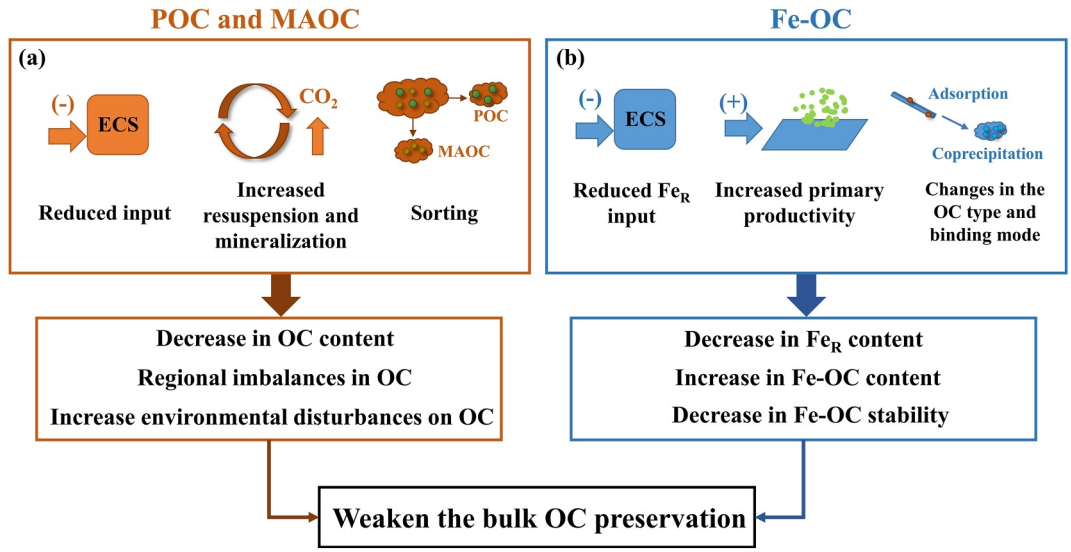

Figure 8. The paradigm of organic carbon fractions under sedimentary environment transformation in the estuarine-inner shelf areas of the East China Sea. (a) Paradigm of POC and MAOC fractions; (b) Paradigm of Fe-OC fractions.

terrestrial sources caused a decrease in inputs of terrestrial OC and Fe_R (Gao et al., 2015, 2019; Wang, Hao, Feng, et al., 2020; Figures 6a and 6d). The resuspension of fine sediments transport further south resulted in a reduction of MAOC and an increase of POC (Figure 8a). Thus, a significant quantity of easily decomposable POC was deposited in the CRE, while the ISR deposited relatively fewer stable MAOC than before, resulting in a disruption of the OC deposition equilibrium (Figure 8a). This renders the OC in the ECS more vulnerable to environmental decomposition. The reduction in Fe_R did not result in a decline in the content of Fe-OC, as the enhanced primary productivity influenced how Fe_R binds OC (Figure 8b). Notwithstanding the elevated Fe-OC content under sedimentary environment transformation, the preservation of OC from terrestrial sources and the enhancement of OC stability by Fe_R appears to be constrained (Figure 8b). It is worth focusing our attention on the fact that the ability of Fe_R to bind terrestrial sources of OC may be decreasing due to watershed changes, reduced Fe_R input, and redox environment which may have unusual implications for the major topic of terrestrial sources of OC deposition in RiOMars (Zhao et al., 2023).

In the long term, the stability and preservation of OC in the ECS will be significantly reduced compared with that before the sedimentary environment transformation. Therefore, we need to pay more attention to the effect of sedimentary environment transformation on OC deposition by different preservation mechanisms in the ECS. While this study attempts to explore the response and various OC preservation mechanisms under the sedimentary environment transformation in the estuarine-inner shelf areas of the ECS, these responses and variations are not restricted to this region. Global deltas are generally at risk of hidden degradation under the combined effects of sharply reduced sediment inputs from terrestrial sources and enhanced regional waves (Zhu et al., 2024). For example, erosion events in the marginal seas of the Shandong Peninsula have affected the compositional characteristics of OC (Che et al., 2024), and sediment resuspension in the Pearl River estuary has increased the rate of OC mineralization (S. Liu et al., 2024). The paradigm proposed in this study is likely to be found in other river-dominated passive margins mainly East Asia, the Mediterranean, and the Gulf Coast (Zhu et al., 2024), such as the Yellow River-Bohai Sea, Nile-Mediterranean Sea and Mississippi River-Gulf of Mexico (L. Liu et al., 2022; Milliman, 1997; Stanley, 1996; Syvitski et al., 2009; Wang et al., 2016). The transformation may lead to changes in the preservation mechanisms of different OC fractions and extended exposure time to oxygen during enhanced resuspension-sedimentation cycles, which could facilitate OC decomposition.

It is worth mentioning that we have only discussed the effect of sedimentary environment transformation on OC deposition at the later transport level. However, a deeper understanding of the vertical process of sedimentary environment transformation on OC deposition is necessary. Moreover, many details in this study are unclear, such as the change of specific chemical composition, degradation characteristics, and ages of the different fractions of OC. More deeper understanding of the specific fate and the long-term variation of OC stability in response to

sedimentary environment transformation needs to be addressed to meet the challenges of global change. Although it has some shortcomings, our study opens up new perspectives for studying the effects of sedimentary environment transformation on OC.

5. Conclusions

This comprehensive analysis of different OC fractions provides a new understanding of the alteration of OC preservation mechanism under sedimentary environment transformation. In ECS, the reduction in inputs from terrestrial sources has resulted in a decline in MAOC content, which has in turn decreased the content and stability of OC. Sedimentary environmental transformation leads to the selective sorting of OC in plant debris and OC associated with minerals, thereby disrupting the equilibrium of OC stability. The contributions of different protective fractions to OC sequestration vary across different regions of the ECS. Notably, Fe-OC plays an enhanced role in OC content under sedimentary environmental transformation, but its contribution to the terrestrial OC and OC ability is low. The conclusions should be extended to other typical RiOMars to test their applicability to other systems. The impact of sedimentary environment transformation on different OC fractions may lead to a weakening of the OC deposition in river-dominated passive-margin continental shelves worldwide.

There are still many unresolved issues, such as the vertical processes of OC fractions under sedimentary environment transformation and the specific fate of different protective mechanisms for OC from different sources. Further research should be conducted on the fate of different OC fractions to examine specific mechanisms of OC preservation by different mechanisms and to investigate the evolutionary processes during long-term burial in river-dominated passive margin areas. In general, this study has opened a new perspective for OC deposition in the ECS, considering the influences of processes at greater depths and strengthening the connection with the actual issues faced by the ECS.

Data Availability Statement

All data in this research are available at Zenodo (https://doi.org/10.5281/zenodo.1395440) (Zhang et al., 2024). Supplementary information data to this article can be found online at https://zenodo.org/records/13954407.

Acknowledgments
The study was supported by Natural Resources Science and Technology Project of Jiangsu Province (JSZRKJ202423), Natural Science Foundation of China (Grant 42106056), Fundamental Research Funds for the Central Universities (Grants 0209-14370410, 0209–14380134), Postgraduate Research & Practice Innovation Program of Jiangsu Province (Grant KYCX24_0199) and the Innovation Platform for Academicians of Hainan Province and its specific research fund (Grant YSPTZX202128).

References

Bao, R., Blattmann, T. M., McIntyre, C., Zhao, M., & Eglinton, T. I. (2019). Relationships between grain size and organic carbon ^{14}C heterogeneity in continental margin sediments. *Earth and Planetary Science Letters*, *505*, 76–85. https://doi.org/10.1016/j.epsl.2018.10.013

Bao, R., van der Voort, T. S., Zhao, M., Guo, X., Montluçon, D. B., McIntyre, C., & Eglinton, T. I. (2018). Influence of hydrodynamic processes on the fate of sedimentary organic matter on continental margins. *Global Biogeochemical Cycles*, *32*(9), 1420–1432. https://doi.org/10.1029/2018gb005921

Bianchi, T. S., & Allison, M. A. (2009). Large-river delta-front estuaries as natural "recorders" of global environmental change. *Proceedings of the National Academy of Sciences*, *106*(20), 8085–8092. https://doi.org/10.1073/pnas.0812878106

Blair, N. E., & Aller, R. C. (2012). The fate of terrestrial organic carbon in the marine environment. *Annual Review of Marine Science*, *4*(1), 401–423. https://doi.org/10.1146/annurev-marine-120709-142717

Blattmann, T. M., Liu, Z., Zhang, Y., Zhao, Y., Haghipour, N., Montluçon, D. B., et al. (2019). Mineralogical control on the fate of continentally derived organic matter in the ocean. *Science*, *366*(6466), 742–745. https://doi.org/10.1126/science.aax5345

Che, Y., Lin, C., Li, S., Liu, J., Zhu, L., Yu, S., et al. (2024). Influences of hydrodynamics on microbial community assembly and organic carbon composition of resuspended sediments in shallow marginal seas. *Water Research*, *248*, 120882. https://doi.org/10.1016/j.watres.2023.120882

Chen, C., Hall, S. J., Coward, E., & Thompson, A. (2020). Iron-mediated organic matter decomposition in humid soils can counteract protection. *Nature Communications*, *11*(1), 2255. https://doi.org/10.1038/s41467-020-16071-5

Cotrufo, M. F., Ranalli, M. G., Haddix, M. L., Six, J., & Lugato, E. (2019). Soil carbon storage is informed by particulate and mineral-associated organic matter. *Nature Geoscience*, *12*(12), 989–994. https://doi.org/10.1038/s41561-019-0484-6

Cui, X., Bianchi, T. S., Hutchings, J. A., Savage, C., & Curtis, J. H. (2016). Partitioning of organic carbon among density fractions in surface sediments of Fiordland, New Zealand. *Journal of Geophysical Research: Biogeosciences*, *121*(3), 1016–1031. https://doi.org/10.1002/2015jg003225

Faust, J. C., Tessin, A., Fisher, B. J., Zindorf, M., Papadaki, S., Hendry, K. R., et al. (2021). Millennial scale persistence of organic carbon bound to iron in Arctic marine sediments. *Nature Communications*, *12*(1), 275. https://doi.org/10.1038/s41467-020-20550-0

Gao, J. H., Jia, J., Kettner, A. J., Xing, F., Wang, Y. P., Li, J., et al. (2018). Reservoir-induced changes to fluvial fluxes and their downstream impacts on sedimentary processes: The Changjiang (Yangtze) River, China. *Quaternary International*, *493*, 187–197. https://doi.org/10.1016/j.quaint.2015.03.015

Gao, J. H., Jia, J., Sheng, H., Yu, R., Li, G. C., Wang, Y. P., et al. (2017). Variations in the transport, distribution, and budget of ^{210}Pb in sediment over the estuarine and inner shelf areas of the East China Sea due to Changjiang catchment changes. *Journal of Geophysical Research: Earth Surface*, *122*(1), 235–247. https://doi.org/10.1002/2016jf004130

Gao, J. H., Jia, J., Wang, Y. P., Yang, Y., Li, J., Bai, F., et al. (2015). Variations in quantity, composition and grain size of Changjiang sediment discharging into the sea in response to human activities. *Hydrology and Earth System Sciences*, *19*(2), 645–655. https://doi.org/10.5194/hess-19-645-2015

Gao, J. H., Shi, Y., Sheng, H., Kettner, A. J., Yang, Y., Jia, J. J., et al. (2019). Rapid response of the Changjiang (Yangtze) River and East China Sea source-to-sink conveying system to human induced catchment perturbations. *Marine Geology*, *414*, 1–17. https://doi.org/10.1016/j.margeo.2019.05.003

Gao, S., & Collins, M. B. (2014). Holocene sedimentary systems on continental shelves. *Marine Geology*, *352*, 268–294. https://doi.org/10.1016/j.margeo.2014.03.021

Gao, S., Wang, D., Yang, Y., Zhou, L., Zhao, Y., Gao, W., et al. (2016). Holocene sedimentary systems on a broad continental shelf with abundant river input: Process–product relationships. *Geological Society, London, Special Publications*, *429*(1), 223–259. https://doi.org/10.1144/sp429.4

Gordon, E. S., & Goñi, M. A. (2003). Sources and distribution of terrigenous organic matter delivered by the Atchafalaya River to sediments in the northern Gulf of Mexico. *Geochimica et Cosmochimica Acta*, *67*(13), 2359–2375. https://doi.org/10.1016/s0016-7037(02)01412-6

He, H., Zhigang, Y., Chen, H., Qingzhen, Y., & Tiezhu, M. (2010). The water elutriator method for particle size seperation and its application. *Periodical of Ocean University of China*, *40*(2), 68–72.

Hu, L., Ji, Y., Zhao, B., Liu, X., Du, J., Liang, Y., & Yao, P. (2023). The effect of iron on the preservation of organic carbon in marine sediments and its implications for carbon sequestration. *Science China Earth Sciences*, *66*(9), 1946–1959. https://doi.org/10.1007/s11430-023-1139-9

Ji, Y., Feng, L., Zhang, D., Wang, Q., Pan, G., & Li, X. (2020). Hydrodynamic sorting controls the transport and hampers source identification of terrigenous organic matter: A case study in East China Sea inner shelf and its implication. *Science of the Total Environment*, *706*, 135699. https://doi.org/10.1016/j.scitotenv.2019.135699

Kleber, M., Eusterhues, K., Keiluweit, M., Mikutta, C., Mikutta, R., & Nico, P. S. (2015). Mineral–organic associations: Formation, properties, and relevance in soil environments. In *Advances in agronomy* (Vol. 130, pp. 1–140). https://doi.org/10.1016/bs.agron.2014.10.005

Lalonde, K., Mucci, A., Ouellet, A., & Gélinas, Y. (2012). Preservation of organic matter in sediments promoted by iron. *Nature*, *483*(7388), 198–200. https://doi.org/10.1038/nature10855

Lavallee, J. M., Soong, J. L., & Cotrufo, M. F. (2020). Conceptualizing soil organic matter into particulate and mineral-associated forms to address global change in the 21st century. *Global Change Biology*, *26*(1), 261–273. https://doi.org/10.1111/gcb.14859

Lee, H. J., & Chao, S. Y. (2003). A climatological description of circulation in and around the East China Sea. *Deep Sea Research Part II: Topical Studies in Oceanography*, *50*(6–7), 1065–1084. https://doi.org/10.1016/s0967-0645(03)00010-9

Li, H. M., Tang, H. J., Shi, X. Y., Zhang, C. S., & Wang, X. L. (2014). Increased nutrient loads from the Changjiang (Yangtze) River have led to increased harmful algal blooms. *Harmful Algae*, *39*, 92–101. https://doi.org/10.1016/j.hal.2014.07.002

Liu, H., Yao, P., Meng, J., Wang, J., & Zhao, B. (2017). Speciation and transformation of phosphorus in surface sediments of the Changjiang Estuary and adjacent shelf based on water elutriation. *Haiyang Xuebao*, *39*(8), 115–128. https://doi.org/10.3969/j.issn.0253-4193.2017.08.011

Liu, J., Saito, Y., Kong, X., Wang, H., Xiang, L., Wen, C., & Nakashima, R. (2010). Sedimentary record of environmental evolution off the Yangtze River estuary, East China Sea, during the last∼ 13,000 years, with special reference to the influence of the Yellow River on the Yangtze River delta during the last 600 years. *Quaternary Science Reviews*, *29*(17–18), 2424–2438. https://doi.org/10.1016/j.quascirev.2010.06.016

Liu, J. P., Li, A. C., Xu, K. H., Velozzi, D. M., Yang, Z. S., Milliman, J. D., & DeMaster, D. J. (2006). Sedimentary features of the Yangtze River-derived along-shelf clinoform deposit in the East China Sea. *Continental Shelf Research*, *26*(17–18), 2141–2156. https://doi.org/10.1016/j.csr.2006.07.013

Liu, J. P., Xu, K. H., Li, A. E. A., Milliman, J. D., Velozzi, D. M., Xiao, S. B., & Yang, Z. S. (2007). Flux and fate of Yangtze River sediment delivered to the East China Sea. *Geomorphology*, *85*(3–4), 208–224. https://doi.org/10.1016/j.geomorph.2006.03.023

Liu, L., Wang, H. J., Yang, Z. S., Fan, Y. Y., Wu, X., Hu, L. M., & Bi, N. S. (2022). Coarsening of sediments from the Huanghe (Yellow River) delta-coast and its environmental implications. *Geomorphology Mar*, *15*, 401.

Liu, S., Gao, Q., Wu, J., Xie, Y., Yang, Q., Wang, R., & Cui, Y. (2024). The concentration of CH_4, N_2O and CO_2 in the Pearl River estuary increased significantly due to the sediment particle resuspension and the interaction of hypoxia. *Science of the Total Environment*, *911*, 168795. https://doi.org/10.1016/j.scitotenv.2023.168795

Lugato, E., Lavallee, J. M., Haddix, M. L., Panagos, P., & Cotrufo, M. F. (2021). Different climate sensitivity of particulate and mineral-associated soil organic matter. *Nature Geoscience*, *14*(5), 295–300. https://doi.org/10.1038/s41561-021-00744-x

Ma, W. W., Zhu, M. X., Yang, G. P., & Li, T. (2018). Iron geochemistry and organic carbon preservation by iron (oxyhydr) oxides in surface sediments of the East China Sea and the south Yellow Sea. *Journal of Marine Systems*, *178*, 62–74. https://doi.org/10.1016/j.jmarsys.2017.10.009

Mehra, O. P., & Jackson, M. L. (2013). Iron oxide removal from soils and clays by a dithionite–citrate system buffered with sodium bicarbonate. In *Clays and clay minerals* (pp. 317–327). Pergamon.

Milliman, J. D. (1997). Blessed dams or damned dams? *Nature*, *386*(6623), 325–327. https://doi.org/10.1038/386325a0

Pan, H. (2016). *Distribution, source and decay of size-fractionated particulate organic carbon in the Changjiang Estuary based on water elutriation* (Doctoral dissertation). Ocean University of China.

Pan, H., Peng, Y., Bin, Z., Jia, M., Dong, L., & Wang, J. (2015). Sources, distribution and preservation of size-fractionated particulate organic carbon in the turbidity maximum zone of the Changjiang Estuary based on water elutriation. *Hai Yang Xue Bao*, *37*(4), 1–15.

Pan, H., Peng, Y., Wang, J., Tingting, Z., Bin, Z., & Dong, L. (2016). Sources, distribution, and decay of size-fractionated paricluate organic carbon in the Changjiang Estuary based on water elutriation. *Periodical of Ocean University of China*, *46*(2), 90–99.

Sheng, A., Liu, J., Li, X., Luo, L., Ding, Y., Chen, C., et al. (2021). Labile Fe (III) supersaturation controls nucleation and properties of product phases from Fe (II)-catalyzed ferrihydrite transformation. *Geochimica et Cosmochimica Acta*, *309*, 272–285. https://doi.org/10.1016/j.gca.2021.06.027

Shields, M. R., Bianchi, T. S., Gélinas, Y., Allison, M. A., & Twilley, R. R. (2016). Enhanced terrestrial carbon preservation promoted by reactive iron in deltaic sediments. *Geophysical Research Letters*, *43*(3), 1149–1157. https://doi.org/10.1002/2015gl067388

Stanley, D. J. (1996). Nile delta: Extreme case of sediment entrapment on a delta plain and consequent coastal land loss. *Marine Geology*, *129*(3–4), 189–195. https://doi.org/10.1016/0025-3227(96)83344-5

Sun, X., Fan, D., Cheng, P., Hu, L., Sun, X., Guo, Z., & Yang, Z. (2021). Source, transport and fate of terrestrial organic carbon from Yangtze River during a large flood event: Insights from multiple-isotopes ($\delta^{13}C$, $\delta^{15}N$, $\Delta^{14}C$) and geochemical tracers. *Geochimica et Cosmochimica Acta*, *308*, 217–236. https://doi.org/10.1016/j.gca.2021.06.004

Sun, X., Hu, L., Fan, D., Wang, H., Yang, Z., & Guo, Z. (2024). Sediment resuspension accelerates the recycling of terrestrial organic carbon at a large river-coastal ocean interface. *Global Biogeochemical Cycles*, *38*(7), e2024GB008213. https://doi.org/10.1029/2024gb008213

Syvitski, J. P., Kettner, A. J., Overeem, I., Hutton, E. W., Hannon, M. T., Brakenridge, G. R., et al. (2009). Sinking deltas due to human activities. *Nature Geoscience*, *2*(10), 681–686. https://doi.org/10.1038/ngeo629

Tesi, T., Semiletov, I., Dudarev, O., Andersson, A., & Gustafsson, Ö. (2016). Matrix association effects on hydrodynamic sorting and degradation of terrestrial organic matter during cross-shelf transport in the Laptev and East Siberian shelf seas. *Journal of Geophysical Research: Biogeosciences*, *121*(3), 731–752. https://doi.org/10.1002/2015jg003067

Vosteen, P., Spiegel, T., Gledhill, M., Frank, M., Zabel, M., & Scholz, F. (2022). The fate of sedimentary reactive iron at the land-ocean interface: A case study from the Amazon shelf. *Geochemistry, Geophysics, Geosystems*, *23*(11), e2022GC010543. https://doi.org/10.1029/2022gc010543

Wagai, R., & Mayer, L. M. (2007). Sorptive stabilization of organic matter in soils by hydrous iron oxides. *Geochimica et Cosmochimica Acta*, *71*(1), 25–35. https://doi.org/10.1016/j.gca.2006.08.047

Wakeham, S. G., Canuel, E. A., Lerberg, E. J., Mason, P., Sampere, T. P., & Bianchi, T. S. (2009). Partitioning of organic matter in continental margin sediments among density fractions. *Marine Chemistry*, *115*(3–4), 211–225. https://doi.org/10.1016/j.marchem.2009.08.005

Wang, C., Hao, Z., Feng, Z., Zhang, C., Gao, J., Li, Y., et al. (2020). Rapid changes in organochlorine pesticides in sediments from the East China Sea and their response to human-induced catchment changes. *Water Research*, *169*, 115225. https://doi.org/10.1016/j.watres.2019.115225

Wang, C., Hao, Z., Gao, J., Feng, Z., Ding, Y., Zhang, C., & Zou, X. (2020). Reservoir construction has reduced organic carbon deposition in the East China Sea by half since 2006. *Geophysical Research Letters*, *47*(17), e2020GL087357. https://doi.org/10.1029/2020gl087357

Wang, C. L., Zhang, C. C., Wang, Y. M., Jia, G. D., Wang, Y. P., Zhu, C., et al. (2022). Anthropogenic perturbations to the fate of terrestrial organic matter in a river-dominated marginal sea. *Geochimica et Cosmochimica Acta*, *333*, 242–262. https://doi.org/10.1016/j.gca.2022.07.012

Wang, J., Peng, Y., Jia, M., Bin, Z., Pan, H., Zhang, T., & Dong, L. (2015). Sources, distribution, and preservation of size-fractionated sedimentary organic carbon of the Changjiang Estuary and adjacent shelf based on water elutriation. *Hai Yang Xue Bao*, *37*(6), 41–57.

Wang, S., Fu, B., Piao, S., Lü, Y., Ciais, P., Feng, X., & Wang, Y. (2016). Reduced sediment transport in the Yellow River due to anthropogenic changes. *Nature Geoscience*, *9*(1), 38–41. https://doi.org/10.1038/ngeo2602

Waterson, E. J., & Canuel, E. A. (2008). Sources of sedimentary organic matter in the Mississippi River and adjacent Gulf of Mexico as revealed by lipid biomarker and δ^{13}CTOC analyses. *Organic Geochemistry*, *39*(4), 422–439. https://doi.org/10.1016/j.orggeochem.2008.01.011

Wu, X. D., Song, J. M., & Li, X. G. (2014). Seasonal variation of water mass characteristic and influence area in the Yangtze Estuary and its adjacent waters. *Marine Science*, *38*, 110–119.

Wu, Y., Eglinton, T., Yang, L., Deng, B., Montluçon, D., & Zhang, J. (2013). Spatial variability in the abundance, composition, and age of organic matter in surficial sediments of the East China Sea. *Journal of Geophysical Research: Biogeosciences*, *118*(4), 1495–1507. https://doi.org/10.1002/2013jg002286

Wu, Y., Zhang, J., Liu, S. M., Zhang, Z. F., Yao, Q. Z., Hong, G. H., & Cooper, L. (2007). Sources and distribution of carbon within the Yangtze River system. *Estuarine, Coastal and Shelf Science*, *71*(1–2), 13–25. https://doi.org/10.1016/j.ecss.2006.08.016

Yang, H. F., Yang, S. L., Xu, K. H., Milliman, J. D., Wang, H., Yang, Z., et al. (2018). Human impacts on sediment in the Yangtze River: A review and new perspectives. *Global and Planetary Change*, *162*, 8–17. https://doi.org/10.1016/j.gloplacha.2018.01.001

Yang, Z. S., Wang, H. J., Saito, Y., Milliman, J. D., Xu, K., Qiao, S., & Shi, G. (2006). Dam impacts on the Changjiang (Yangtze) River sediment discharge to the sea: The past 55 years and after the Three Gorges Dam. *Water Resources Research*, *42*(4). https://doi.org/10.1029/2005wr003970

Yao, P., Yu, Z., Bianchi, T. S., Guo, Z., Zhao, M., Knappy, C. S., et al. (2015). A multiproxy analysis of sedimentary organic carbon in the Changjiang Estuary and adjacent shelf. *Journal of Geophysical Research: Biogeosciences*, *120*(7), 1407–1429. https://doi.org/10.1002/2014jg002831

Ye, C., Chen, D., Hall, S. J., Pan, S., Yan, X., Bai, T., et al. (2018). Reconciling multiple impacts of nitrogen enrichment on soil carbon: Plant, microbial and geochemical controls. *Ecology Letters*, *21*(8), 1162–1173. https://doi.org/10.1111/ele.13083

Zhang, Z. Y., Wang, C. L., & Zou, X. Q. (2024). Divergent responses of organic carbon to sedimentary environment transformation in a River-dominated Marginal Sea (version v3) [Dataset]. *Zenodo*. https://doi.org/10.5281/zenodo.13353965

Zhao, B., Yao, P., Bianchi, T. S., Shields, M. R., Cui, X., Zhang, X., et al. (2018). The role of reactive iron in the preservation of terrestrial organic carbon in estuarine sediments. *Journal of Geophysical Research: Biogeosciences*, *123*(12), 3556–3569. https://doi.org/10.1029/2018jg004649

Zhao, B., Yao, P., Bianchi, T. S., Wang, X., Shields, M. R., Schröder, C., & Yu, Z. (2023). Preferential preservation of pre-aged terrestrial organic carbon by reactive iron in estuarine particles and coastal sediments of a large river-dominated estuary. *Geochimica et Cosmochimica Acta*, *345*, 34–49. https://doi.org/10.1016/j.gca.2023.01.023

Zhao, B., Yao, P., Bianchi, T. S., & Yu, Z. G. (2021). Controls on organic carbon burial in the Eastern China marginal seas: A regional synthesis. *Global Biogeochemical Cycles*, *35*(4), e2020GB006608. https://doi.org/10.1029/2020gb006608

Zhu, Q., Xing, F., Wang, Y. P., Syvitski, J., Overeem, I., Guo, J., et al. (2024). Hidden delta degradation due to fluvial sediment decline and intensified Maine storms. *Science Advances*, *10*(18), eadk1698. https://doi.org/10.1126/sciadv.adk1698

References From the Supporting Information

Wang, C. L., Zou, X. Q., Zhao, Y. F., Li, Y. L., Song, Q. C., Wang, T., & Yu, W. W. (2017). Distribution pattern and mass budget of sedimentary polycyclic aromatic hydrocarbons in shelf areas of the Eastern China Marginal Seas. *Journal of Geophysical Research: Oceans*, *122*(6), 4990–5004. https://doi.org/10.1002/2017jc012890